Shell evolution of $N = 40$ isotones towards ^{60}Ca: First spectroscopy of ^{62}Ti

M.L. Cortés, W. Rodriguez, P. Doornenbal, A. Obertelli, J.D. Holt, S.M. Lenzi, J. Menéndez, F. Nowacki, K. Ogata, A. Poves, et al.

Physics Letters B 800 (2020) 135071

Contents lists available at ScienceDirect

Physics Letters B

www.elsevier.com/locate/physletb

Shell evolution of $N = 40$ isotones towards ^{60}Ca: First spectroscopy of ^{62}Ti

M.L. Cortés [a,b,*], W. Rodriguez [c,a], P. Doornenbal [a], A. Obertelli [d,e], J.D. Holt [f], S.M. Lenzi [g], J. Menéndez [h], F. Nowacki [i], K. Ogata [j,k], A. Poves [l], T.R. Rodríguez [l], A. Schwenk [e,m,n], J. Simonis [o], S.R. Stroberg [f,p], K. Yoshida [q], L. Achouri [r], H. Baba [a], F. Browne [a], D. Calvet [d], F. Château [d], S. Chen [s,a], N. Chiga [a], A. Corsi [d], A. Delbart [d], J.-M. Gheller [d], A. Giganon [d], A. Gillibert [d], C. Hilaire [d], T. Isobe [a], T. Kobayashi [t], Y. Kubota [a,h], V. Lapoux [d], H.N. Liu [d,e,u], T. Motobayashi [a], I. Murray [v,a], H. Otsu [a], V. Panin [a], N. Paul [d], H. Sakurai [a,w], M. Sasano [a], D. Steppenbeck [a], L. Stuhl [h], Y.L. Sun [d,e], Y. Togano [x], T. Uesaka [a], K. Wimmer [w], K. Yoneda [a], O. Aktas [u], T. Aumann [e,y], L.X. Chung [z], F. Flavigny [v], S. Franchoo [v], I. Gašparić [aa,a], R.-B. Gerst [ab], J. Gibelin [r], K.I. Hahn [ac], D. Kim [ac], T. Koiwai [w], Y. Kondo [ad], P. Koseoglou [e,y], J. Lee [ae], C. Lehr [e], B.D. Linh [z], T. Lokotko [ae], M. MacCormick [v], K. Moschner [ab], T. Nakamura [ad], S.Y. Park [ac], D. Rossi [e], E. Sahin [af], D. Sohler [ag], P.-A. Söderström [e], S. Takeuchi [ad], H. Toernqvist [e,y], V. Vaquero [ah], V. Wagner [e], S. Wang [ai], V. Werner [e], X. Xu [ae], H. Yamada [ad], D. Yan [ai], Z. Yang [a], M. Yasuda [ad], L. Zanetti [e]

[a] *RIKEN Nishina Center, 2-1 Hirosawa, Wako, Saitama 351-0198, Japan*
[b] *Istituto Nazionale di Fisica Nucleare, Laboratori Nazionali di Legnaro, I-35020 Legnaro, Italy*
[c] *Universidad Nacional de Colombia, Sede Bogota, Facultad de Ciencias, Departamento de Física, Bogotá, 111321, Colombia*
[d] *IRFU, CEA, Université Paris-Saclay, F-91191 Gif-sur-Yvette, France*
[e] *Institut für Kernphysik, Technische Universität Darmstadt, 64289 Darmstadt, Germany*
[f] *TRIUMF, 4004 Wesbrook Mall, Vancouver BC V6T 2A3, Canada*
[g] *Dipartimento di Fisica e Astronomia, Università di Padova and INFN, Sezione di Padova, Via F. Marzolo 8, I-35131 Padova, Italy*
[h] *Center for Nuclear Study, The University of Tokyo, RIKEN campus, Wako, Saitama 351-0198, Japan*
[i] *IPHC, CNRS/IN2P3, Université de Strasbourg, F-67037 Strasbourg, France*
[j] *Research Center for Nuclear Physics (RCNP), Osaka University, Ibaraki 567-0047, Japan*
[k] *Department of Physics, Osaka City University, Osaka 558-8585, Japan*
[l] *Departamento de Física Teórica and IFT-UAM/CSIC, Universidad Autónoma de Madrid, E-2804 Madrid, Spain*
[m] *ExtreMe Matter Institute EMMI, GSI Helmholtzzentrum für Schwerionenforschung GmbH, 64291 Darmstadt, Germany*
[n] *Max-Planck-Institut für Kernphysik, Saupfercheckweg 1, 69117 Heidelberg Germany*
[o] *Institut für Kernphysik and PRISMA Cluster of Excellence, Johannes Gutenberg-Universität, Mainz 55099, Germany*
[p] *Department of Physics, University of Washington, Seattle WA, USA*
[q] *Advanced Science Research Center, Japan Atomic Energy Agency, Tokai, Ibaraki 319-1195, Japan*
[r] *LPC Caen, ENSICAEN, Université de Caen, CNRS/IN2P3, F-14050 Caen, France*
[s] *State Key Laboratory of Nuclear Physics and Technology, Peking University, Beijing 100871, PR China*
[t] *Department of Physics, Tohoku University, Sendai 980-8578, Japan*
[u] *Department of Physics, Royal Institute of Technology, SE-10691 Stockholm, Sweden*
[v] *IPN Orsay, CNRS and Université Paris Saclay, F-91406 Orsay Cedex, France*
[w] *Department of Physics, University of Tokyo, 7-3-1 Hongo, Bunkyo, Tokyo 113-0033, Japan*
[x] *Department of Physics, Rikkyo University, 3-34-1 Nishi-Ikebukuro, Toshima, Tokyo 172-8501, Japan*
[y] *GSI Helmholtzzentrum für Schwerionenforschung GmbH, Planckstr. 1, 64291 Darmstadt, Germany*
[z] *Institute for Nuclear Science & Technology, VINATOM, P.O. Box 5T-160, Nghia Do, Hanoi, Viet Nam*
[aa] *Ruđer Bošković Institute, Bijenička cesta 54,10000 Zagreb, Croatia*
[ab] *Institut für Kernphysik, Universität zu Köln, D-50937 Cologne, Germany*
[ac] *Department of Science Education and Department of Physics, Ewha Womans University, Seoul 03760, Republic of Korea*
[ad] *Department of Physics, Tokyo Institute of Technology, 2-12-1 O-Okayama, Meguro, Tokyo, 152-8551, Japan*
[ae] *Department of Physics, The University of Hong Kong, Pokfulam, Hong Kong*
[af] *Department of Physics, University of Oslo, N-0316 Oslo, Norway*

* Corresponding author at: Istituto Nazionale di Fisica Nucleare, Laboratori Nazionali di Legnaro, I-35020 Legnaro, Italy.
E-mail address: liliana.cortes@lnl.infn.it (M.L. Cortés).

https://doi.org/10.1016/j.physletb.2019.135071

[ag] Institute for Nuclear Research of the Hungarian Academy of Sciences (MTA Atomki), P.O. Box 51, Debrecen H-4001, Hungary
[ah] Instituto de Estructura de la Materia, CSIC, E-28006 Madrid, Spain
[ai] Institute of Modern Physics, Chinese Academy of Sciences, Lanzhou, PR China

ARTICLE INFO

Article history:
Received 17 September 2019
Received in revised form 29 October 2019
Accepted 29 October 2019
Available online 4 November 2019
Editor: D.F. Geesaman

Keywords:
Shell evolution
Radioactive beams
Gamma-ray spectroscopy

ABSTRACT

Excited states in the $N = 40$ isotone ^{62}Ti were populated via the ^{63}V$(p, 2p)^{62}$Ti reaction at ∼200 MeV/nucleon at the Radioactive Isotope Beam Factory and studied using γ-ray spectroscopy. The energies of the $2_1^+ \rightarrow 0_{gs}^+$ and $4_1^+ \rightarrow 2_1^+$ transitions, observed here for the first time, indicate a deformed ^{62}Ti ground state. These energies are increased compared to the neighboring ^{64}Cr and ^{66}Fe isotones, suggesting a small decrease of quadrupole collectivity. The present measurement is well reproduced by large-scale shell-model calculations based on effective interactions, while ab initio and beyond mean-field calculations do not yet reproduce our findings. The shell-model calculations for ^{62}Ti show a dominant configuration with four neutrons excited across the $N = 40$ gap. Likewise, they indicate that the $N = 40$ island of inversion extends down to $Z = 20$, disfavoring a possible doubly magic character of the elusive ^{60}Ca.

Our understanding of atomic nuclei largely derives from the concept of nuclear shell structure. Within this picture, the arrangement of nucleons inside the nucleus can be explained by the filling of discrete energy levels. Sizable gaps between these orbits disfavor the population of the higher-energy levels, and are interpreted as closed shells, which give rise to magic numbers. Such shell closures can be evidenced by a relatively high-lying first excited 2^+ state, a relatively small electric quadrupole transition probability to the ground state, $B(E2)\downarrow$, and a steep decrease of the separation energy. Experimental evidence collected in the last decades, particularly since the advent of radioactive ion beams, has shown that shell structure undergoes significant changes for isotopes far from stability [1]. Examples of these changes are the appearance of new magic neutron numbers at $N = 32, 34$ in the Ca isotopes and neighboring isotopic chains [2–9], and at $N = 16$ for O isotopes [10–12], as well as the disappearance of the shell closure at $N = 8$ [13–16], $N = 20$ [17,18] and $N = 28$ [19,20] in various neutron-rich isotopes.

Given that $N = 40$, which corresponds to the filling of the neutron pf shells, is a harmonic oscillator magic number, the study of the structure of $N = 40$ isotones can provide insight into the mechanisms governing shell evolution. Indeed the characteristics of this isotonic chain vary with the number of protons. For ^{68}Ni ($Z = 28$), a high $E(2_1^+)$ energy and a low $B(E2)\downarrow$ have been observed [21]. However, due to the parity change between the pf shell and the $g_{9/2}$ orbit, the 2_1^+ state involves at least two neutrons across $N = 40$. Such a neutron-dominated excitation could result in a large $E(2_1^+)$ energy and low $B(E2)\downarrow$ value without a large shell gap [22]. For the neutron-rich Fe ($Z = 26$) and Cr ($Z = 24$) isotopes, a monotonous decrease of the $E(2_1^+)$ when approaching $N = 40$ and beyond has been observed [23–26]. This decrease indicates a rapid development of collectivity when removing protons from the $f_{7/2}$ shell. In contrast, the measurement of the $E(2_1^+)$ of ^{58,60}Ti ($Z = 22$) only showed a moderate decrease towards $N = 40$ [27,28]. The very exotic ^{60}Ca ($Z = 20$), where the Ca isotopic chain meets the $N = 40$ isotones, is a key nucleus for shell evolution [29,30], but difficult to reach experimentally. Only recently its existence has been established [31], supporting theoretical predictions for a bound ^{70}Ca. However, the heaviest Ca isotope with known spectroscopic information is ^{54}Ca [4].

Theoretical calculations in the shell-model framework [32] concluded that the development of collectivity in $N = 40$ nuclei is due to quadrupole correlations that give rise to deformed ground states, dominated by intruder neutron orbits beyond the pf shell. This leads to an island of inversion below ^{68}Ni, similar to the one formed around ^{32}Mg [32]. These calculations predict an increase in the $E(2_1^+)$ energy of the more exotic $N = 40$ isotones ^{62}Ti and ^{60}Ca, while conserving the intruder character in the ground state. On the other hand, symmetry conserving configuration mixing calculations with the Gogny interaction predict a conservation of the $N = 40$ gap [33]. These results agree with calculations performed using the five-dimension collective Hamiltonian, which suggest an energy gap of about 4 MeV at $N = 40$, predicting spherical ^{62}Ti and ^{60}Ca [34,35]. It is noted that the beyond-mean-field and the shell model calculations provide similar results for ^{64}Cr and ^{66}Fe, while they substantially diverge for ^{60}Ca and ^{62}Ti. Therefore, spectroscopy of ^{62}Ti offers a crucial test between the two different pictures. In addition, the properties of Ca isotopes have been extensively studied with coupled-cluster theory [36] and valence-shell interactions [3,37], in both cases using two-nucleon (NN) and three-nucleon (3N) interactions from chiral effective field theory. Such calculations agree well with experimental energy levels and binding energies up to ^{54}Ca, and predict the drip line to be located around ^{60}Ca. This is in contrast to density functional theories based on the mean field approach which predict, depending on the selected interaction, Ca isotopes to be bound up to $A = 68 - 76$. Beyond $N = 40$, coupled-cluster theory suggests the existence of two-neutron halos and Efimov states in ^{62}Ca [38].

Clearly, spectroscopic information on exotic isotopes around ^{60}Ca is necessary to deepen our understanding of the nuclear structure at $N = 40$ and to benchmark the theoretical predictions towards the neutron drip line. In the present work, the first spectroscopy of ^{62}Ti is presented. This isotope represents the closest nucleus to ^{60}Ca for which spectroscopic studies can be performed at existing radioactive beam facilities.

The experiment was carried out at the Radioactive Isotope Beam Factory, operated by the RIKEN Nishina Center and the Center for Nuclear Study of the University of Tokyo. A primary beam of ^{70}Zn with an energy of 345 MeV/nucleon and an average intensity of 240 pnA was fragmented on a 3-mm thick Be target to produce a cocktail of secondary beams which included ^{63}V. The fragments of interest were selected with the $B\rho - \Delta E - B\rho$ technique using two wedge-shaped aluminium degraders situated at the dispersive focal planes of BigRIPS [39]. Event-by-event identification was performed by an energy loss measurement in an ionization chamber, position and angle measurements in parallel plate avalanche counters at different focal planes, and the time-of-flight measured between two plastic scintillators. The ^{63}V isotopes were

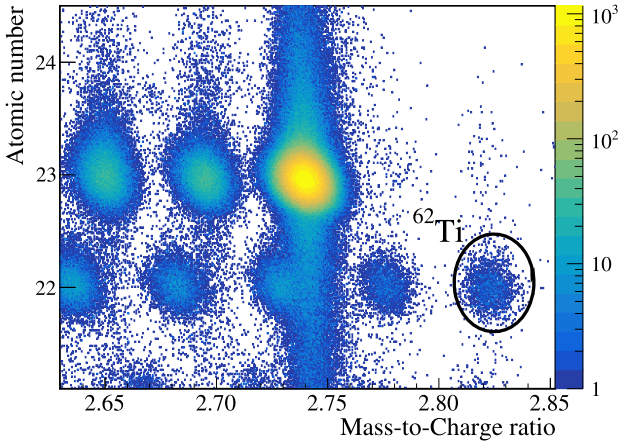

Fig. 1. Particle identification plot for the outgoing fragments measured with the SAMURAI dipole magnet and related detectors. Incoming ^{63}V isotopes were selected with BigRIPS. ^{62}Ti isotopes are indicated by the ellipse.

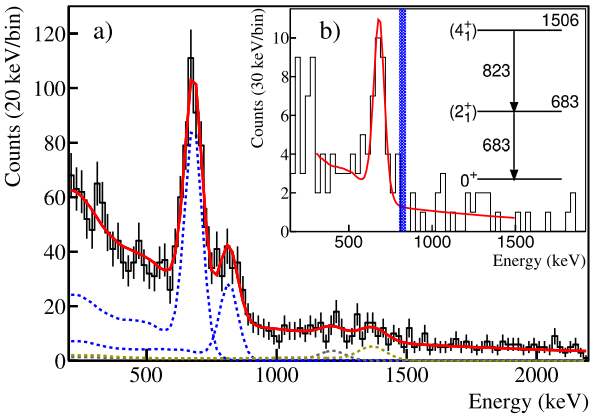

Fig. 2. a) Doppler corrected γ-ray spectrum of ^{62}Ti obtained from proton knockout from ^{63}V. The spectrum was fitted by the convolution of the simulated response of DALI2$^+$ to the observed transitions and a double exponential background. Two additional transitions are included to improve the fit (see text for details). b) Coincidence spectrum obtained when applying the gate indicated by the blue area.

delivered to the focus area in front of the SAMURAI dipole magnet [40], with an average intensity of 3 pps and an average energy of 239 MeV/nucleon. At this location the MINOS device [41], composed of a 151.3(13) mm long liquid hydrogen target surrounded by a Time Projection Chamber (TPC), was placed. The efficiency of MINOS to detect at least one proton was measured as 93(4)% and the resolution for the vertex reconstruction was estimated to be better than 2 mm (σ) [42]. Following proton knockout reactions in the liquid hydrogen target, the ^{62}Ti fragments had an average energy of 154 MeV/nucleon and were identified using the SAMURAI dipole magnet and associated detectors [40]. Fig. 1 shows the particle identification obtained with SAMURAI when selecting ^{63}V as incoming beam. A total of 1880 events corresponding to the ^{63}V$(p,2p)^{62}$Ti reaction was reconstructed. The transmission of the unreacted ^{63}V beam along the beam line was measured to be 50.9(11)% and the inclusive $(p,2p)$ cross section was determined to be 4.0(1) mb.

MINOS was surrounded by the high-efficiency γ-ray detector array DALI2$^+$, composed of 226 NaI(Tl) detectors covering angles between $\sim$15° and $\sim$118° with respect to the center of the target [43,44]. The array was energy calibrated using standard ^{60}Co, ^{88}Y, ^{133}Ba, and ^{137}Cs sources. The full-energy-peak efficiency of the array was determined using a detailed GEANT4 [45] simulation and was found to be 30% at 1 MeV with an energy resolution of 11% for a source moving at 0.6c.

Doppler corrected γ-ray spectra were obtained using the reaction vertex and the velocity of the fragment reconstructed with MINOS. Peak-to-total ratio and detection efficiency improved by adding-up the energies of γ-rays deposited in detectors up to 10 cm apart. To avoid the reconstruction of add-back events from the large atomic background, γ-rays with energies below 100 keV were not taken into account in the analysis. The Doppler corrected spectrum obtained for the ^{63}V$(p,2p)^{62}$Ti reaction is displayed in Fig. 2a). Two peaks are clearly visible and the $\gamma-\gamma$ coincidence analysis demonstrates their coincidence (Fig. 2b). Using a 2-dimensional χ^2 minimization, the energies of the transitions were deduced to be 683(10) keV and 823(20) keV. In this minimization procedure, the simulated response of DALI2$^+$ to transitions of different energies were fitted in steps of 5 keV to the experimental data and the χ^2 value was obtained for each combination of energies. The simulation included the experimental resolution of each crystal and a double exponential background was assumed for the fit. The parameters of these exponential functions were chosen based on a consistent analysis of the spectra of proton knockout reactions producing ^{50}Ar and ^{60}Ti. The errors on the transition energies include the statistical error from the fit, as well as the systematic error arising from the calibration of the γ-ray detectors and the possible lifetime of the states. Given that global systematic fits [46] suggest a lifetime of the 2_1^+ state below 30 ps, an uncertainty of 15 ± 15 ps was considered for the decay of the 2_1^+, while the 4_1^+ was considered short lived. The best total fit as well as the individual response functions of DALI2$^+$ are shown in Fig. 2. The relative intensities of the peaks suggest the tentative assignment of the 683(10) keV and the 823(20) keV peaks to the $2_1^+ \rightarrow 0_{gs}^+$ and $4_1^+ \rightarrow 2_1^+$ transitions, respectively.

A structure in the γ-ray spectrum above the estimated background was observed between 1000 and 1500 keV. Two additional transitions at energies of 1222(37) keV and 1328(45) keV, were used to reproduce this structure. The significance levels of these peaks are 2σ and 3σ, respectively. The inclusion of more transitions did not provide any further improvement on the χ^2 of the fit. A structure at 320 keV was observed with a significance level of 1σ. The existence of this peak could not be firmly established, therefore it was not considered, and its possible contribution to the partial cross section was assumed to be within the error bars of the analysis. These possible transitions indicate the presence of different states being populated in the reaction, but the limited resolution of DALI2$^+$ and the low statistics did not allow to identify them nor to perform a coincidence analysis. The existence of such transitions, which potentially feed the 2_1^+ or 4_1^+ states, implies a fragmented spectroscopic strength.

Exclusive cross sections to populate the (2_1^+) and (4_1^+) states, from which additional feeding should be subtracted, were calculated based on the fitted γ-ray intensities, the total transmission of the isotopes and the efficiency of MINOS. Cross sections of 1.5(3) mb and 0.8(1) mb were obtained for the (2_1^+) state and the (4_1^+) state, respectively. The cross sections measured for the possible transitions at 1222(37) keV and 1328(45) keV were determined to be 0.2(1) mb and 0.3(1) mb, respectively. As no firm statement can be made regarding these transitions, we limit the interpretation to their possible direct feeding to the 2_1^+ state. For this, the average value between 100% feeding and no feeding was considered and the error increased to cover both possibilities, giving a exclusive cross section of 1.3(4) mb for the (2_1^+) state.

The evolution of measured $E(2_1^+)$ and $E(4_1^+)$ energies for the $N = 40$ isotones between Ti and Ge [47] is presented in Fig. 3. The $E(2_1^+)$ and $E(4_1^+)$ reported in this Letter for ^{62}Ti have a similar value than the ones measured for ^{66}Fe, higher than those of

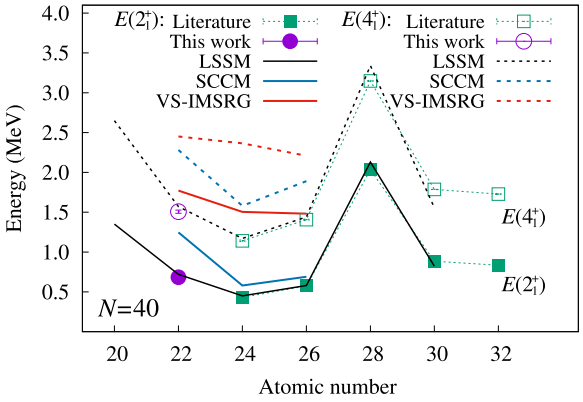

Fig. 3. Systematics of $E(2_1^+)$ (filled symbols) and $E(4_1^+)$ (open symbols) for even-even $N = 40$ isotones. The circles represent the present measurement. The black, blue, and red lines represent LSSM, SCCM, and VS-IMSRG calculations, respectively (see text for details).

^{64}Cr. It is pointed out that ^{64}Cr, with a $E(2_1^+)$ of 420 keV, has the largest quadrupole deformation observed in the region [26,48]. Our results show the first increase of $E(2_1^+)$ along the $N = 40$ isotones towards ^{60}Ca. This increase establishes a parabolic trend and suggests a decrease in quadrupole collectivity. This, in turn, could be interpreted as a sign of a significant $N = 40$ shell gap, and gives the possibility of a doubly magic character for ^{60}Ca.

Large Scale Shell Model (LSSM) calculations, shown by the black lines in Fig. 3, were carried out with the LNPS interaction [32] using a ^{48}Ca core and a valence space which included the full pf shell for protons and the $0f_{5/2}$, $1p_{3/2}$, $1p_{1/2}$, $0g_{9/2}$, and $1d_{5/2}$ orbits for neutrons. This interaction has already successfully reproduced the $E(2_1^+)$ of the heavier $N = 40$ isotones [32]. The LSSM calculations reproduce very accurately the data for both the $E(2_1^+)$ and $E(4_1^+)$ of the $N = 40$ isotones including our values for ^{62}Ti. This agreement strengthens the tentative spin and parity assignment for these states. As shown in Ref. [32], the calculations predict a reduction of the $0f_{5/2} - 0g_{9/2}$ gap when going from ^{68}Ni to ^{60}Ca, as well as the closeness of the quadrupole partner orbits $0g_{9/2}$ and $1d_{5/2}$. Due to this proximity, quadrupole correlations produce a gain in energy that largely overcomes the cost of exciting neutrons across the $N = 40$ gap, thereby favoring many-particle-many-hole configurations. This situation resembles the behavior at $N = 20$ and suggests an island of inversion for $N = 40$ isotones below ^{68}Ni. For ^{62}Ti, a gap of about 1 MeV is predicted, with a resulting wave function dominated by 4p-4h excitations (63%) and a significant 6p-6h component (22%) [32]. Furthermore, a ground-state deformation parameter $\beta = 0.28$ for ^{62}Ti is obtained. The agreement with the measured energies of the $N = 40$ isotones, including ^{62}Ti, indicates that the island of inversion in this region extends down to ^{60}Ca. It is particularly remarkable that although the $E(2_1^+)$ for ^{60}Ca is predicted to be 1.35 MeV, which represents an increase with respect to the neighboring isotones, a 4p-4h configuration dominance (59%) prevails [32].

Symmetry conserving configuration mixing (SCCM) calculations using the Gogny D1S effective interaction [49,50] were performed for ^{62}Ti, ^{64}Cr, and ^{66}Fe, and are indicated by the blue lines in Fig. 3. For the calculations, each individual nuclear state was defined as the linear combination of multiple intrinsic many-body states with different quadrupole (axial and triaxial) shapes [51,33]. Cranked or octupole deformed states were not included, therefore, a systematic stretching of the levels with respect to the experimental values is expected [52,53]. The $E(2_1^+)$ predicted for ^{64}Cr and ^{66}Fe lie very close to the LSSM predictions, and are in fair agreement with the experimental data. However, when going to ^{62}Ti, a more abrupt increase of the $E(2_1^+)$ is obtained. For the $E(4_1^+)$ energies, the calculations overestimate the experimental values by about 500 keV, although the minimum value for ^{64}Cr is maintained. It is noted that for ^{64}Cr and ^{66}Fe, where the deformation is well described by the model, the inclusion of cranking would further improve the agreement with the experimental data. Within this model, the energy gap at $N = 40$ is conserved, leading to a ground state of ^{62}Ti highly mixed with the spherical configuration. This is also the case for ^{60}Ca, which is predicted as a doubly magic nucleus with an $E(2_1^+)$ of 4.73 MeV [53]. It is noted that although this calculation yields a spherical ground state for ^{62}Ti, the 2_1^+ and 4_1^+ states belong to a deformed band starting at the 0_2^+ state. This band can correspond to the predictions of the LSSM calculations and indicate that the SCCM calculations overestimate the $N = 40$ gap in this region.

Ab initio valence-space in-medium similarity renormalization group (VS-IMSRG) [54–58] calculations were also performed for ^{62}Ti, ^{64}Cr, and ^{66}Fe, as shown by the red lines in Fig. 3. The chiral NN+3N interaction labeled 1.8/2.0 (EM) in Refs. [59,60] was used, which is based on the NN potential from Ref. [61] and 3N forces fitted to light systems up to ^{4}He only. With this NN+3N interaction, ground-state energies up to Sn [58,59,62,63] are generally well reproduced. As the VS-IMSRG captures 3N forces between valence nucleons via an ensemble normal ordering [57], a separate valence-space interaction is decoupled for each nucleus of interest. Here, the same model space as the LNPS Hamiltonian is considered (adding the $2s_{1/2}$ neutron orbital for ^{62}Ti). Using the Magnus formulation of the IMSRG [64], operators at the two-body level are truncated in the so-called IMSRG(2) approximation. The VS-IMSRG interaction is diagonalized with the code ANTOINE [65], including, for the first time in the VS-IMSRG, both intruder quadrupole partners, such as $0g_{9/2}$–$1d_{5/2}$ [66]. The VS-IMSRG overestimates the $E(2_1^+)$ and $E(4_1^+)$ excitation energies in ^{62}Ti, ^{64}Cr, and ^{66}Fe, predicting all states as spherical. Cross-shell excitations to the $0g_{9/2}$–$1d_{5/2}$ orbits stay at the 1p-1h level because of the substantial $N = 40$ shell gap, 3.7 MeV in ^{62}Ti. Within this model, a $E(2_1^+)$ of around 7 MeV is predicted for ^{60}Ca, an overestimation which is also observed at other shell closures with the VS-IMSRG [59,63,67]. This limitation has been related to the IMSRG(2) truncation [66], which may not fully capture correlations associated with cross-shell excitations. Preliminary comparisons with coupled-cluster theory indicate that keeping operators at the three-body level will improve the results. Also, choosing a deformed reference state, instead of spherical as in the present work, may capture quadrupole correlations more efficiently [68,69].

Single-particle theoretical cross sections were computed in the DWIA framework [70]. The single-particle wave functions and the nuclear density were obtained by the Bohr-Mottelson single-particle potential [71]. The optical potentials for the distorted waves in the initial and final channels were constructed by the microscopic folding model [72] with the Melbourne G-matrix interaction [73] and with the calculated nuclear density. The spin-orbit part of each distorting potential was disregarded. As for the transition interaction, the Franey-Love effective proton-proton interaction was adopted [74]. Cross sections at different beam energies, from 240 MeV/nucleon at the entrance of the target to 154 MeV/nucleon at the exit, were calculated and weighted according to the energy loss in the target. Theoretical cross sections (σ_{theo}) were obtained by weighting the single particle cross sections by the calculated spectroscopic factors.

The spin and parity of the ground state of ^{63}V are not known experimentally. The LSSM calculation suggests it to be $3/2^-$, although states with spin and parity of $5/2^-$ and $7/2^-$ appear very close in energy, suggesting the presence of isomeric states. No ex-

Table 1
Experimentally deduced excitation energies and cross sections for ^{62}Ti following the ^{63}V$(p,2p)^{62}$Ti reaction, and comparison with theoretical cross sections obtained with the LSSM calculation. The spectroscopic factors and corresponding cross sections are shown for the three possible values of the spin and parity of the ground state of ^{63}V. The experimental ground-state cross section was calculated by subtracting the cross sections of the measured transitions from the inclusive cross section.

E (keV)	σ_{exp} (mb)	E (keV)	J^π	l_j	$\sigma_{s.p}$ (mb)	$J^\pi = 3/2^-$		$J^\pi = 5/2^-$		$J^\pi = 7/2^-$	
						C^2S	σ_{theo} (mb)	C^2S	σ_{theo} (mb)	C^2S	σ_{theo} (mb)
0	1.4(4)	0	0_1^+	$p_{3/2}$	1.56	0.03	0.05	–	0.04	–	0.58
				$f_{7/2}$	1.46	–		0.03		0.4	
683(10)	1.3(4)	720	2_1^+	$p_{3/2}$	1.54	0.06	0.61	0.01	0.97	0.02	0.07
				$f_{7/2}$	1.44	0.36		0.66		0.03	
1506(22)	0.8(1)	1570	4_1^+	$p_{3/2}$	1.50	–	1.30	0.04	0.38	0.04	0.44
				$f_{7/2}$	1.41	0.92		0.23		0.27	

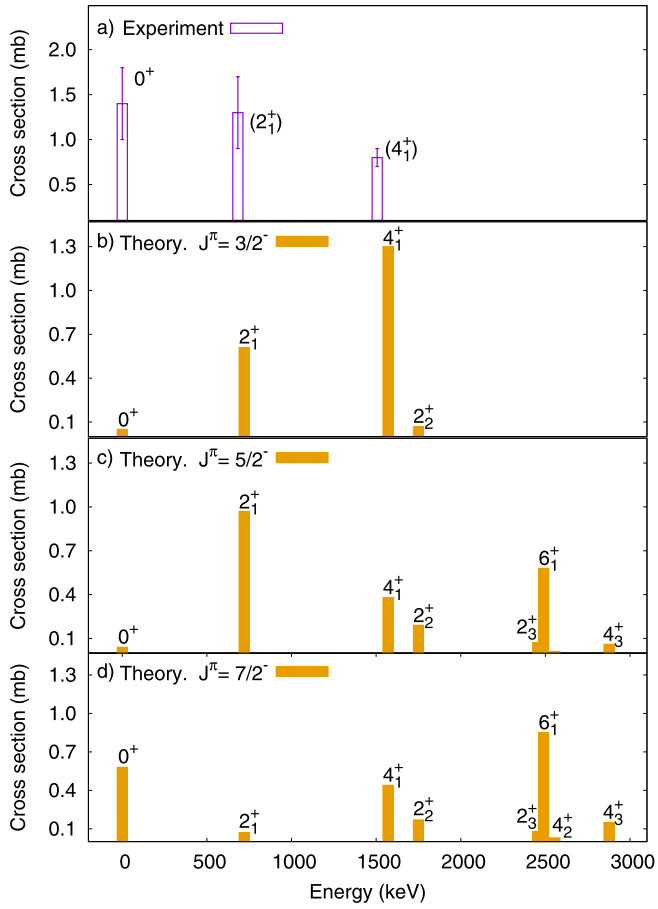

Fig. 4. Partial proton removal cross sections for the ^{63}V$(p,2p)^{62}$Ti reaction. Panel a) shows the experimental results. Panels b) to d) show LSSM calculations using the LNPS interaction assuming the ground state of ^{63}V as $3/2^-$, $5/2^-$ and $7/2^-$, respectively.

perimental evidence of such states has been reported so far and available data are consistent with a $3/2^-$ assignment [75]. Results of the calculations for the three cases are shown in Table 1, and displayed in Fig. 4, together with the experimental results. It can be seen that neither the absolute value or the general trend shown by the data are reproduced by the calculation in any scenario. The calculation for the ground state of $J^\pi = 3/2^-$ resembles better the experimental data in terms of the number of states that are populated, while for the cases of $J^\pi = 5/2^-$ and $J^\pi = 7/2^-$ a considerable population of the 6_1^+ state would be expected. In particular for the case of $J^\pi = 7/2^-$ a population of the 6_1^+ state higher than the one of the 2_1^+ state would be expected, at odds with the experimental result. It is noted that the calculated spectroscopic factors add up to less than half of the total strength in the three cases. Therefore, population of higher lying states is expected by the calculations. Such a scenario would lead to unobserved transitions feeding the 4_1^+ or the 2_1^+ states directly, which can account for the excess of the measured cross section in comparison with the calculations. Although not in good agreement, the low measured and calculated partial cross sections, as well as the apparent fragmentation of the spectroscopic strength, are consistent with the collective nature of the ^{62}Ti ground state discussed in this work. However, the large error bars prevent a firmer conclusion.

In summary, first spectroscopy of ^{62}Ti was obtained by means of the ^{63}V$(p,2p)^{62}$Ti reaction at ∼200 MeV/nucleon. Transitions at 683(10) keV and 823(20) keV were assigned to the decay of the 2_1^+ and 4_1^+ states at 683(10) keV and 1506(22) keV, respectively. Our result shows for the first time an increase of the $E(2_1^+)$ for $N = 40$ isotones towards ^{60}Ca. LSSM calculations were in good agreement with the experimental findings. The calculations suggest that although the collectivity decreases approaching ^{60}Ca, with an ensuing increase of $E(2_1^+)$, quadrupole correlation contributions remain and lead to the extension of the $N = 40$ island of inversion down to ^{60}Ca. SCCM calculations overestimate the measured $E(2_1^+)$ and $E(4_1^+)$ of ^{62}Ti, predicting a doubly magic character of ^{60}Ca and a weakly deformed ground state in ^{62}Ti, at variance with the LSSM calculations. For these calculations the $N = 40$ spherical gap is too large to produce the inversion between the quasi-spherical and deformed 0^+ states. VS-IMSRG calculations, which provide a good description of excited states in Ca isotopes, largely overestimate the $E(2_1^+)$ and $E(4_1^+)$ energies of ^{62}Ti, even after the inclusion of the neutron $0g_{9/2}$, $1d_{5/2}$ and $2s_{1/2}$ orbitals. The spectroscopic information presented in this Letter offers an important benchmark for our understanding of nuclear structure approaching ^{60}Ca and the location of the neutron drip line.

We thank the RIKEN Nishina Center accelerator staff and the BigRIPS team for the stable operation of the high-intensity Zn beam and for the preparation of the secondary beam setting. K.O. acknowledges the support by Grant-in-Aid for Scientific Research of the Japan Society for the Promotion of Science (JSPS) JP16K05352. A.P. is supported in part by the Ministerio de Ciencia, Innovación y Universidades (Spain), Severo Ochoa Programme SEV-2016-0597 and grant PGC-2018-94583. F.B. is supported by the RIKEN Special Postdoctoral Researcher Program. L.X.C. and B.D.L. would like to thank the Vietnam Ministry of Science and Technology (MOST) for its support through the Physics Development Program Grant No. ĐTĐLCN.25/18. I.G. has been supported by HIC for FAIR and Croatian Science Foundation under projects no. 1257 and 7194. D. So. was supported by the the European Regional Development Fund contract No. GINOP-2.3.3-15-2016-00034 and the National Research, Development and Innovation Fund of Hungary via Project No. K128947. V.V. acknowledges support from the Spanish Ministerio de Economía y Competitividad under Contract No. FPA2017-84756-C4-2-P. K.I.H., D.K. and S.Y.P. acknowledge the support from the National Research Foundation of Korea grant No.

2018R1A5A1025563 and 2019M7A1A1033186. The development of MINOS was supported by the European Research Council through the ERC Grant No. MINOS-258567. This work was also supported by the JSPS KAKENHI Grant No. 18K03639, MEXT as "Priority issue on post-K computer" (Elucidation of the fundamental laws and evolution of the universe), the Joint Institute for Computational Fundamental Science (JICFuS), the CNS-RIKEN joint project for large-scale nuclear structure calculations, Natural Sciences and Engineering Research Council (NSERC) of Canada, the Deutsche Forschungsgemeinschaft – Projektnummer 279384907 – SFB 1245, the PRISMA Cluster of Excellence, and the BMBF under Contracts No. 05P18RDFN1 and 05P19RDFN1. TRIUMF receives funding via a contribution through the National Research Council Canada. Computations were performed at the Jülich Supercomputing Center (JURECA).

References

[1] O. Sorlin, M.-G. Porquet, Prog. Part. Nucl. Phys. 61 (2008) 602–673, https://doi.org/10.1016/j.ppnp.2008.05.001. URL: http://www.sciencedirect.com/science/article/pii/S0146641008000380.
[2] A. Gade, et al., Phys. Rev. C 74 (2006) 021302, https://doi.org/10.1103/PhysRevC.74.021302. URL: http://link.aps.org/doi/10.1103/PhysRevC.74.021302.
[3] F. Wienholtz, et al., Nature 498 (2013) 346–349, https://doi.org/10.1038/nature12226.
[4] D. Steppenbeck, et al., Nature 502 (2013) 207–210, https://doi.org/10.1038/nature12522.
[5] D. Steppenbeck, et al., Phys. Rev. Lett. 114 (2015) 252501, https://doi.org/10.1103/PhysRevLett.114.252501. URL: https://link.aps.org/doi/10.1103/PhysRevLett.114.252501.
[6] M. Rosenbusch, et al., Phys. Rev. Lett. 114 (2015) 202501, https://doi.org/10.1103/PhysRevLett.114.202501. URL: https://link.aps.org/doi/10.1103/PhysRevLett.114.202501.
[7] E. Leistenschneider, et al., Phys. Rev. Lett. 120 (2018) 062503, https://doi.org/10.1103/PhysRevLett.120.062503. URL: https://link.aps.org/doi/10.1103/PhysRevLett.120.062503.
[8] S. Michimasa, et al., Phys. Rev. Lett. 121 (2018) 022506, https://doi.org/10.1103/PhysRevLett.121.022506. URL: https://link.aps.org/doi/10.1103/PhysRevLett.121.022506.
[9] H.N. Liu, et al., Phys. Rev. Lett. 122 (2019) 072502, https://doi.org/10.1103/PhysRevLett.122.072502. URL: https://link.aps.org/doi/10.1103/PhysRevLett.122.072502.
[10] A. Ozawa, et al., Phys. Rev. Lett. 84 (2000) 5493–5495, https://doi.org/10.1103/PhysRevLett.84.5493. URL: http://link.aps.org/doi/10.1103/PhysRevLett.84.5493.
[11] A. Obertelli, et al., Phys. Lett. B 633 (2006) 33–37, https://doi.org/10.1016/j.physletb.2005.11.033. URL: http://www.sciencedirect.com/science/article/pii/S0370269305017016.
[12] R. Kanungo, et al., Phys. Rev. Lett. 102 (2009) 152501, https://doi.org/10.1103/PhysRevLett.102.152501. URL: http://link.aps.org/doi/10.1103/PhysRevLett.102.152501.
[13] A. Navin, et al., Phys. Rev. Lett. 85 (2000) 266–269, https://doi.org/10.1103/PhysRevLett.85.266. URL: http://link.aps.org/doi/10.1103/PhysRevLett.85.266.
[14] H. Iwasaki, et al., Phys. Lett. B 481 (2000) 7–13, https://doi.org/10.1016/S0370-2693(00)00428-7. URL: http://www.sciencedirect.com/science/article/pii/S0370269300004287.
[15] H. Iwasaki, et al., Phys. Lett. B 491 (2000) 8–14, https://doi.org/10.1016/S0370-2693(00)01017-0. URL: http://www.sciencedirect.com/science/article/pii/S0370269300010170.
[16] S. Shimoura, et al., Phys. Lett. B 560 (2003) 31–36, https://doi.org/10.1016/S0370-2693(03)00341-1. URL: http://www.sciencedirect.com/science/article/pii/S0370269303003411.
[17] C. Détraz, et al., Phys. Rev. C 19 (1979) 164–176, https://doi.org/10.1103/PhysRevC.19.164. URL: https://link.aps.org/doi/10.1103/PhysRevC.19.164.
[18] T. Motobayashi, et al., Phys. Lett. B 346 (1995) 9–14, https://doi.org/10.1016/0370-2693(95)00012-A. URL: http://www.sciencedirect.com/science/article/pii/037026939500012A.
[19] B. Bastin, et al., Phys. Rev. Lett. 99 (2007) 022503, https://doi.org/10.1103/PhysRevLett.99.022503. URL: http://link.aps.org/doi/10.1103/PhysRevLett.99.022503.
[20] S. Takeuchi, et al., Phys. Rev. Lett. 109 (2012) 182501, https://doi.org/10.1103/PhysRevLett.109.182501. URL: http://link.aps.org/doi/10.1103/PhysRevLett.109.182501.
[21] O. Sorlin, et al., Phys. Rev. Lett. 88 (2002) 092501, https://doi.org/10.1103/PhysRevLett.88.092501. URL: http://link.aps.org/doi/10.1103/PhysRevLett.88.092501.
[22] K. Langanke, et al., Phys. Rev. C 67 (2003) 044314, https://doi.org/10.1103/PhysRevC.67.044314. URL: https://link.aps.org/doi/10.1103/PhysRevC.67.044314.
[23] M. Hannawald, et al., Phys. Rev. Lett. 82 (1999) 1391–1394, https://doi.org/10.1103/PhysRevLett.82.1391. URL: https://link.aps.org/doi/10.1103/PhysRevLett.82.1391.
[24] P. Adrich, et al., Phys. Rev. C 77 (2008) 054306, https://doi.org/10.1103/PhysRevC.77.054306. URL: https://link.aps.org/doi/10.1103/PhysRevC.77.054306.
[25] C. Santamaria, et al., Phys. Rev. Lett. 115 (2015) 192501, https://doi.org/10.1103/PhysRevLett.115.192501.
[26] A. Gade, et al., Phys. Rev. C 81 (2010) 051304, https://doi.org/10.1103/PhysRevC.81.051304. URL: https://link.aps.org/doi/10.1103/PhysRevC.81.051304.
[27] H. Suzuki, et al., Phys. Rev. C 88 (2013) 024326, https://doi.org/10.1103/PhysRevC.88.024326. URL: https://link.aps.org/doi/10.1103/PhysRevC.88.024326.
[28] A. Gade, et al., Phys. Rev. Lett. 112 (2014) 112503, https://doi.org/10.1103/PhysRevLett.112.112503. URL: https://link.aps.org/doi/10.1103/PhysRevLett.112.112503.
[29] Long Range Plan 2017: Perspectives in Nuclear Physics, Nuclear Physics European Collaboration Committee, 2017.
[30] Reaching for the Horizon. The 2015 Long Range Plan for Nuclear Science, Nuclear Science Advisory Committee, 2015.
[31] O.B. Tarasov, et al., Phys. Rev. Lett. 121 (2018) 022501, https://doi.org/10.1103/PhysRevLett.121.022501. URL: https://link.aps.org/doi/10.1103/PhysRevLett.121.022501.
[32] S.M. Lenzi, et al., Phys. Rev. C 82 (2010) 054301, https://doi.org/10.1103/PhysRevC.82.054301. URL: https://link.aps.org/doi/10.1103/PhysRevC.82.054301.
[33] T.R. Rodríguez, A. Poves, F. Nowacki, Phys. Rev. C 93 (2016) 054316, https://doi.org/10.1103/PhysRevC.93.054316. URL: https://link.aps.org/doi/10.1103/PhysRevC.93.054316.
[34] L. Gaudefroy, et al., Phys. Rev. C 80 (2009) 064313, https://doi.org/10.1103/PhysRevC.80.064313. URL: https://link.aps.org/doi/10.1103/PhysRevC.80.064313.
[35] S. Péru, M. Martini, Eur. Phys. J. A 50 (2014) 88, https://doi.org/10.1140/epja/i2014-14088-7. URL: https://doi.org/10.1140/epja/i2014-14088-7.
[36] G. Hagen, et al., Phys. Rev. Lett. 109 (2012) 032502, https://doi.org/10.1103/PhysRevLett.109.032502. URL: https://link.aps.org/doi/10.1103/PhysRevLett.109.032502.
[37] J.D. Holt, et al., Phys. Rev. C 90 (2014) 024312, https://doi.org/10.1103/PhysRevC.90.024312. URL: https://link.aps.org/doi/10.1103/PhysRevC.90.024312.
[38] G. Hagen, et al., Phys. Rev. Lett. 111 (2013) 132501, https://doi.org/10.1103/PhysRevLett.111.132501. URL: https://link.aps.org/doi/10.1103/PhysRevLett.111.132501.
[39] T. Kubo, et al., Prog. Theor. Exp. Phys. 2012 (2012). URL: http://ptep.oxfordjournals.org/content/2012/1/03C003.abstract.
[40] T. Kobayashi, et al., Nucl. Instrum. Methods Phys. Res. B 317 (2013) 294–304, https://doi.org/10.1016/j.nimb.2013.05.089. URL: http://www.sciencedirect.com/science/article/pii/S0168583X13007118.
[41] A. Obertelli, et al., Eur. Phys. J. A 50 (2014). URL: https://doi.org/10.1140/epja/i2014-14008-y.
[42] C. Santamaria, et al., Nucl. Instrum. Methods Phys. Res. A 905 (2018) 138–148, https://doi.org/10.1016/j.nima.2018.07.053. URL: http://www.sciencedirect.com/science/article/pii/S016890021830888X.
[43] S. Takeuchi, et al., Nucl. Instrum. Methods Phys. Res. A 763 (2014) 596–603, https://doi.org/10.1016/j.nima.2014.06.087. URL: http://www.sciencedirect.com/science/article/pii/S0168900214008419.
[44] I. Murray, et al., RIKEN Accel. Prog. Rep. 51 (2017) 158.
[45] S. Agostinelli, et al., Nucl. Instrum. Methods Phys. Res. A 506 (2003) 250–303, https://doi.org/10.1016/S0168-9002(03)01368-8. URL: http://www.sciencedirect.com/science/article/pii/S0168900203013688.
[46] S. Raman, C. Nestor, P. Tikkanen, At. Data Nucl. Data Tables 78 (2001) 1–128, https://doi.org/10.1006/adnd.2001.0858. URL: http://www.sciencedirect.com/science/article/pii/S0092640X01908587.
[47] http://www.nndc.bnl.gov/ensdf/.
[48] H.L. Crawford, et al., Phys. Rev. Lett. 110 (2013) 242701, https://doi.org/10.1103/PhysRevLett.110.242701. URL: https://link.aps.org/doi/10.1103/PhysRevLett.110.242701.
[49] J. Dechargé, D. Gogny, Phys. Rev. C 21 (1980) 1568–1593, https://doi.org/10.1103/PhysRevC.21.1568. URL: https://link.aps.org/doi/10.1103/PhysRevC.21.1568.
[50] J. Berger, M. Girod, D. Gogny, Nucl. Phys. A 428 (1984) 23–36, https://doi.org/10.1016/0375-9474(84)90240-9. URL: http://www.sciencedirect.com/science/article/pii/0375947484902409.
[51] T.R. Rodríguez, J.L. Egido, Phys. Rev. C 81 (2010) 064323, https://doi.org/10.1103/PhysRevC.81.064323. URL: https://link.aps.org/doi/10.1103/PhysRevC.81.064323.
[52] M. Borrajo, T.R. Rodríguez, J.L. Egido, Phys. Lett. B 746 (2015) 341–346, https://doi.org/10.1016/j.physletb.2015.05.030. URL: http://www.sciencedirect.com/science/article/pii/S0370269315003676.

[53] L.M. Robledo, T.R. Rodríguez, R.R. Rodríguez-Guzmán, J. Phys. G 46 (2018) 013001, https://doi.org/10.1088/1361-6471/aadebd.
[54] K. Tsukiyama, S.K. Bogner, A. Schwenk, Phys. Rev. C 85 (2012) 061304, https://doi.org/10.1103/PhysRevC.85.061304. URL: https://link.aps.org/doi/10.1103/PhysRevC.85.061304.
[55] S.K. Bogner, et al., Phys. Rev. Lett. 113 (2014) 142501, https://doi.org/10.1103/PhysRevLett.113.142501. URL: https://link.aps.org/doi/10.1103/PhysRevLett.113.142501.
[56] S.R. Stroberg, et al., Phys. Rev. C 93 (2016) 051301, https://doi.org/10.1103/PhysRevC.93.051301. URL: https://link.aps.org/doi/10.1103/PhysRevC.93.051301.
[57] S.R. Stroberg, et al., Phys. Rev. Lett. 118 (2017) 032502, https://doi.org/10.1103/PhysRevLett.118.032502. URL: https://link.aps.org/doi/10.1103/PhysRevLett.118.032502.
[58] S.R. Stroberg, et al., arXiv e-prints, arXiv:1902.06154, 2019, arXiv:1902.06154.
[59] J. Simonis, et al., Phys. Rev. C 96 (2017) 014303, https://doi.org/10.1103/PhysRevC.96.0141303. URL: https://link.aps.org/doi/10.1103/PhysRevC.96.014303.
[60] K. Hebeler, et al., Phys. Rev. C 83 (2011) 031301, https://doi.org/10.1103/PhysRevC.83.031301. URL: https://link.aps.org/doi/10.1103/PhysRevC.83.031301.
[61] D.R. Entem, R. Machleidt, Phys. Rev. C 68 (2003) 041001, https://doi.org/10.1103/PhysRevC.68.041001. URL: https://link.aps.org/doi/10.1103/PhysRevC.68.041001.
[62] J. Simonis, et al., Phys. Rev. C 93 (2016) 011302, https://doi.org/10.1103/PhysRevC.93.011302. URL: https://link.aps.org/doi/10.1103/PhysRevC.93.011302.
[63] T.D. Morris, et al., Phys. Rev. Lett. 120 (2018) 152503, https://doi.org/10.1103/PhysRevLett.120.152503. URL: https://link.aps.org/doi/10.1103/PhysRevLett.120.152503.
[64] T.D. Morris, N.M. Parzuchowski, S.K. Bogner, Phys. Rev. C 92 (2015) 034331, https://doi.org/10.1103/PhysRevC.92.034331. URL: https://link.aps.org/doi/10.1103/PhysRevC.92.034331.
[65] E. Caurier, et al., Rev. Mod. Phys. 77 (2005) 427–488, https://doi.org/10.1103/RevModPhys.77.427. URL: https://link.aps.org/doi/10.1103/RevModPhys.77.427.
[66] M. Mougeot, et al., Phys. Rev. Lett. 120 (2018) 232501, https://doi.org/10.1103/PhysRevLett.120.232501. URL: https://link.aps.org/doi/10.1103/PhysRevLett.120.232501.
[67] R. Taniuchi, et al., Nature 569 (2019) 53–58, https://doi.org/10.1038/s41586-019-1155-x. URL: https://doi.org/10.1038/s41586-019-1155-x.
[68] H. Hergert, et al., J. Phys. Conf. Ser. 1041 (2018) 012007, https://doi.org/10.1088/1742-6596/1041/1/012007.
[69] J.M. Yao, et al., Phys. Rev. C 98 (2018) 054311, https://doi.org/10.1103/PhysRevC.98.054311. URL: https://link.aps.org/doi/10.1103/PhysRevC.98.054311.
[70] T. Wakasa, K. Ogata, T. Noro, Prog. Part. Nucl. Phys. 96 (2017) 32–87, https://doi.org/10.1016/j.ppnp.2017.06.002. URL: http://www.sciencedirect.com/science/article/pii/S0146641017300558.
[71] A. Bohr, B.R. Mottelson, Nuclear Structure, vol. 1, 1 ed., W. A. Benjamin, 1969.
[72] M. Toyokawa, K. Minomo, M. Yahiro, Phys. Rev. C 88 (2013) 054602, https://doi.org/10.1103/PhysRevC.88.054602. URL: https://link.aps.org/doi/10.1103/PhysRevC.88.054602.
[73] K. Amos, et al., Adv. Nucl. Phys. 25 (2000) 275.
[74] M.A. Franey, W.G. Love, Phys. Rev. C 31 (1985) 488–498, https://doi.org/10.1103/PhysRevC.31.488. URL: https://link.aps.org/doi/10.1103/PhysRevC.31.488.
[75] S. Suchyta, et al., Phys. Rev. C 89 (2014) 034317, https://doi.org/10.1103/PhysRevC.89.034317. URL: https://link.aps.org/doi/10.1103/PhysRevC.89.034317.